LETTERS

Subcapsular sinus macrophages in lymph nodes clear lymph-borne viruses and present them to antiviral B cells

Tobias Junt[1], E. Ashley Moseman[1], Matteo Iannacone[1,3], Steffen Massberg[1], Philipp A. Lang[4], Marianne Boes[2], Katja Fink[5], Sarah E. Henrickson[1], Dmitry M. Shayakhmetov[6], Nelson C. Di Paolo[6], Nico van Rooijen[7], Thorsten R. Mempel[1], Sean P. Whelan[8] & Ulrich H. von Andrian[1]

Lymph nodes prevent the systemic dissemination of pathogens such as viruses that infect peripheral tissues after penetrating the body's surface barriers. They are also the staging ground of adaptive immune responses to pathogen-derived antigens[1,2]. It is unclear how virus particles are cleared from afferent lymph and presented to cognate B cells to induce antibody responses. Here we identify a population of CD11b$^+$CD169$^+$MHCII$^+$ macrophages on the floor of the subcapsular sinus (SCS) and in the medulla of lymph nodes that capture viral particles within minutes after subcutaneous injection. Macrophages in the SCS translocated surface-bound viral particles across the SCS floor and presented them to migrating B cells in the underlying follicles. Selective depletion of these macrophages compromised local viral retention, exacerbated viraemia of the host, and impaired local B-cell activation. These findings indicate that CD169$^+$ macrophages have a dual physiological function. They act as innate 'flypaper' by preventing the systemic spread of lymph-borne pathogens and as critical gatekeepers at the lymph–tissue interface that facilitate the recognition of particulate antigens by B cells and initiate humoral immune responses.

We have investigated how virus particles that enter peripheral tissues are handled within draining lymph nodes. Hind footpads of mice were injected with fluorescently labelled ultraviolet-inactivated vesicular stomatitis virus (VSV), a cytopathic rhabdovirus that is transmissible by insect bites[3] and elicits T-independent neutralizing B-cell responses[4]. Using multiphoton intravital microscopy (MP-IVM) in popliteal lymph nodes[5] draining the injected footpad, we observed that VSV accumulated in discrete patches on the SCS floor within minutes after subcutaneous injection, whereas the parenchyma and roof of the SCS remained free of virus (Fig. 1a and Supplementary Movie 1). The viral deposits became progressively denser, forming conspicuous irregular reticular patterns, which remained fixed in place for hours.

To characterize the tissue origin of the preferred VSV binding sites in lymph nodes, we reconstituted irradiated Act(EGFP) mice with wild-type bone marrow. The resulting C57BL/6→Act(EGFP) chimaeras expressed enhanced green fluorescent protein (EGFP) in non-haematopoietic cells, particularly lymphatic endothelial cells, on the SCS floor and roof. On injection of fluorescent VSV into the footpad of C57BL/6→Act(EGFP) chimaeras, viral particles flooded the SCS (Supplementary Movie 2). After 3 h, unbound luminal VSV had disappeared, but the SCS floor displayed prominent patches of VSV that did not colocalize with EGFP$^+$ cells, suggesting that VSV was captured by haematopoietic cells (Fig. 1b and Supplementary Movie 3). To characterize the putative VSV-capturing leukocytes, we performed electron microscopy on popliteal lymph nodes harvested 5 min after injection of VSV (Fig. 1c). Bullet-shaped, electron-dense VSV particles were selectively bound to discrete regions on the surface of scattered large cells residing within the SCS or just below the SCS floor. VSV-binding cells that were located beneath the SCS floor were typically in contact with the lymph compartment through protrusions that extended into the SCS lumen.

Ultrastructural studies of lymph nodes have shown that the SCS contains many macrophages[6,7], so we examined whether the VSV-retaining cells belonged to this population. Indeed, confocal microscopy of frozen lymph node sections obtained 30 min after injection into the footpad showed that VSV colocalized in the SCS with a macrophage marker, CD169/sialoadhesin (Fig. 1d). Using flow cytometry, we detected CD169 on about 1–2% of mononuclear cells in lymph nodes, which uniformly expressed CD11b and MHC-II together, indicating that the VSV-binding cells are indeed macrophages (Supplementary Fig. 1). Most CD169$^+$ cells also expressed other macrophage markers, including CD68 and F4/80, but few expressed the granulocyte/monocyte marker Gr-1. CD169$^+$ cells also expressed CD11c, but at lower levels than CD11c^{high} conventional dendritic cells. We conclude that intact virions enter the lymph within minutes after transcutaneous deposition and accumulate rapidly and selectively on macrophages in the medulla and SCS of draining lymph nodes.

To explore mechanisms for virus fixation, live VSV (20 μg containing 2×10^8 plaque-forming units) was injected into hind footpads, and viral titres in draining lymph nodes were assessed 2 h later. There was no defect in VSV retention in draining lymph nodes of mice deficient in complement C3 (Fig. 1e). DH-LMP2a mice, which lack secreted immunoglobulins, had decreased virus titres in spleen but not in popliteal lymph nodes (Fig. 1f). VSV fixation in lymph nodes therefore occurs by means of a mechanism distinct from that used by splenic marginal-zone macrophages, which require C3 and natural antibodies to capture blood-borne VSV[8,9]. Conceivably, the VSV surface glycoprotein may be recognized in lymph nodes by macrophage-expressed carbohydrate-binding scavenger receptors[10], but the precise mechanism will require further investigation.

What are the consequences of viral capture by macrophages for virus dissemination and antiviral immunity? To address this question, we depleted lymph-node-resident macrophages by injection of

[1]Immune Disease Institute and Department of Pathology, Harvard Medical School, [2]Department of Dermatology, Brigham and Women's Hospital, 77 Avenue Louis Pasteur, Boston, Massachusetts 02115, USA. [3]Immunopathogenesis of Liver Infections Unit, San Raffaele Scientific Institute, Via Olgettina 58, 20132 Milan, Italy. [4]Institute of Experimental Immunology, Zurich University Hospital, Schmelzbergstrasse 12, CH-8091 Zurich, Switzerland. [5]Novartis Institute of Tropical Diseases, 10 Biopolis Road, 138670 Singapore. [6]Division of Medical Genetics, Department of Medicine, University of Washington, Seattle, Washington 98195, USA. [7]Vrije Universiteit, VUMC, Department of Molecular Cell Biology, Faculty of Medicine, Van der Boechorststraat 7, 1081 BT Amsterdam, The Netherlands. [8]Department of Microbiology and Molecular Genetics, Harvard Medical School, 200 Longwood Avenue, Boston, Massachusetts 02115, USA.

clodronate liposomes (CLL) into the footpad[11]. At the dose used, subcutaneously injected CLL selectively eliminated macrophages in lymph nodes draining the injection site, including the popliteal, inguinal and para-aortic lymph nodes[11], whereas macrophages in distal lymph nodes and spleen were spared (Supplementary Fig. 2a, b). Among the different lymph-node-resident $CD11b^{+}MHCII^{+}$ phagocytes, CLL preferentially removed the $CD169^{+}$ subset, whereas $LYVE\text{-}1^{+}$ cells and conventional dendritic cells remained unchanged. CLL-treated popliteal lymph nodes had increased B-cell numbers and enlarged follicles seven days after treatment, but other morphological parameters, for example demarcation of the T/B border and the SCS ultrastructure, remained unaltered (Supplementary Fig. 2c–e).

In comparison with untreated lymph nodes, we recovered about tenfold lower viral titres from the draining lymph nodes of CLL-treated mice (Fig. 1g), suggesting that macrophage depletion rendered lymph filtration inefficient. Indeed, VSV titres were markedly increased in blood, spleen and non-draining lymph nodes of CLL-treated mice. Viral dissemination from the injection site to the blood depended strictly on lymph drainage, because circulating VSV was undetectable when virus was injected into footpads of mice that carried an occluding catheter in the thoracic duct, even in CLL-treated mice. Viral titres were low but detectable in thoracic-duct lymph fluid of untreated mice, but increased significantly in CLL-treated animals (Fig. 1h). This indicates that the principal conduit for early viral dissemination from peripheral tissues is the lymph, which is monitored by lymph-node-resident, CLL-sensitive macrophages that prevent the systemic spread of lymph-borne VSV.

This capture mechanism was not unique to VSV: $CD169^{+}$ SCS macrophages also retained adenovirus (Supplementary Fig. 3a–c) and vaccinia virus (Supplementary Fig. 3d), indicating that macrophages act as guardians against many structurally distinct pathogens. In contrast, virus-sized latex beads (200 nm diameter) were poorly retained in the SCS after injection into the footpad (Supplementary Fig. 3e). SCS macrophages therefore discriminate between lymph-borne viruses and other particles of similar size. Fluorescent VSV, adenovirus and vaccinia virus also accumulated in the medulla of draining lymph nodes, where they were bound not only by $CD169^{low}$ cells (Fig. 1d) but also by $CD169^{-}LYVE\text{-}1^{+}$ lymphatic endothelial cells (Supplementary Fig. 3c, d). This was corroborated in CLL-treated lymph nodes, in which VSV accumulated exclusively on medullary $LYVE\text{-}1^{+}$ cells (Supplementary Fig. 4).

Next we examined how captured VSV is recognized by B cells. Popliteal lymph nodes contain rare B cells in the SCS lumen (Supplementary Fig. 5a), but we found no evidence for virus-binding lymphocytes within the SCS on electron micrographs (not shown).

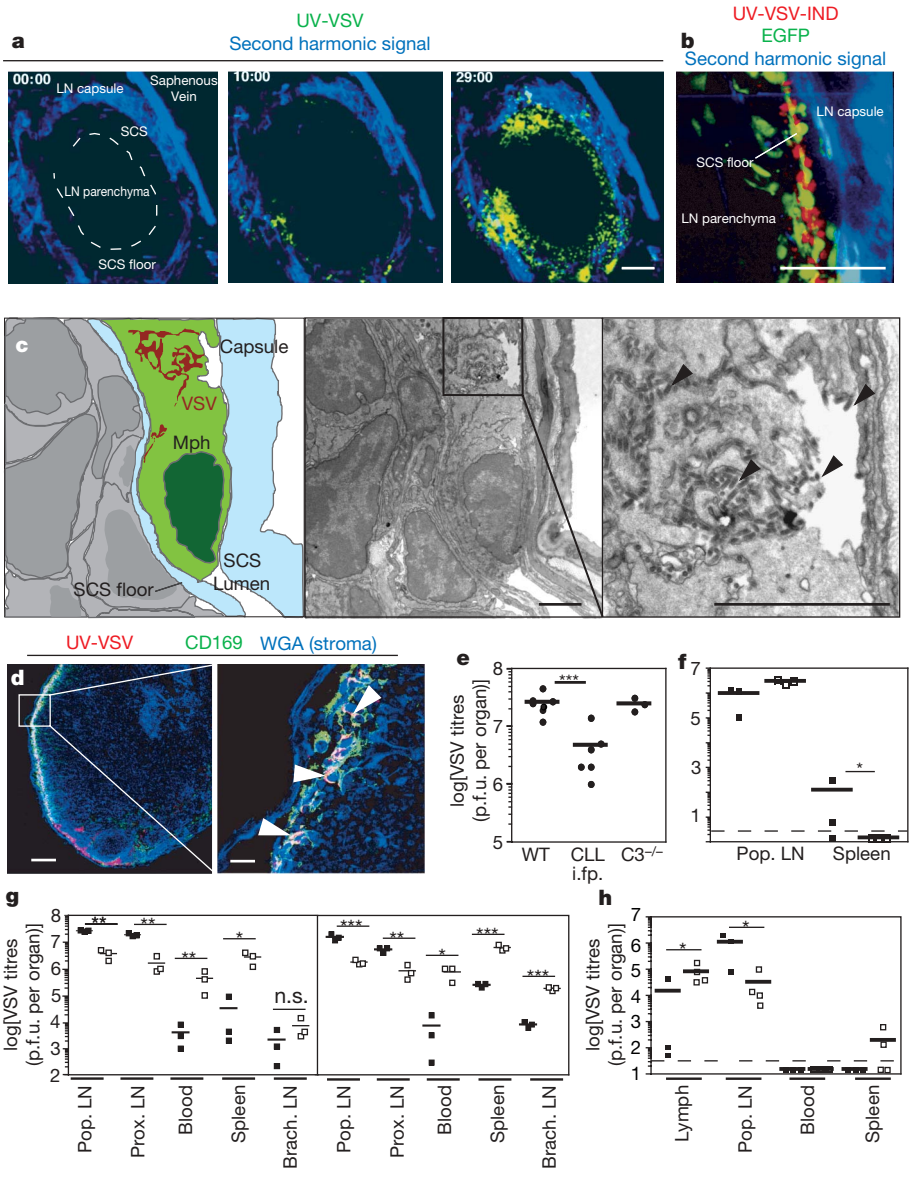

Figure 1 | Capture of lymph-borne VSV by SCS macrophages. **a**, MP-IVM micrographs of VSV (green) in a popliteal lymph node (LN). Numbers indicate minutes after footpad injection. UV-VSV, ultraviolet-inactivated VSV. Scale bar, 100 μm. **b**, VSV (red) accumulation in a C57BL/6→Act(EGFP) recipient 3 h after injection. Scale bar, 50 μm. **c**, Electron micrographs of VSV in lymph node 5 min after injection. The middle micrograph is shown schematically on the left and at higher magnification on the right. Arrowheads identify VSV particles. Scale bars, 2 μm. Mph, macrophage. **d**, Confocal micrographs of VSV-draining lymph node (30 min). Wheatgerm agglutinin (WGA, blue) was used to stain stromal components. Scale bars, 100 μm (left), 15 μm (right). **e**, VSV titres in popliteal lymph nodes 2 h after injection into wild-type mice (WT), C3-deficient mice or macrophage-depleted WT mice that received CLL injections into a footpad (CLL i.fp.). Three asterisks, $P < 0.001$ (two-way ANOVA, Bonferroni's post-test). p.f.u., plaque-forming units. **f**, VSV capture in Balb/c (filled squares) and DH-LMP2a (open squares) mice. Asterisk, $P < 0.05$ (unpaired *t*-test). **g**, VSV titres after footpad injection in untreated (filled squares) and CLL-treated (open squares) mice (one of two similar experiments; $n = 3$). Left, 2 h; right, 6 h. Pop. LN, popliteal lymph node; Prox. LN, inguinal, para-aortic lymph nodes; Brach. LN, brachial lymph node. Asterisk, $P < 0.05$; two asterisks, $P < 0.01$; three asterisks, $P < 0.001$; n.s., not significant (unpaired *t*-test). **h**, Viral titres in lymph, spleen and blood after cannulation of the thoracic duct in untreated (filled squares) and CLL-treated (open squares) mice. Asterisk, $P < 0.05$ (unpaired *t*-test). Horizontal bars in **e**–**h** indicate means.

Instead, viral particles were presented to B cells within superficial follicles by macrophages that extended across the SCS floor. After injection of either VSV (Fig. 2a) or adenovirus (Supplementary Fig. 5b–e), virions were readily detectable at B-cell–macrophage interfaces for at least 4 h. This suggested that SCS macrophages shuttle viral particles across the SCS floor for presentation to B cells. Transcytosis seemed unlikely because the few vesicles containing VSV in SCS macrophages showed evidence of viral degradation. In addition, we did not detect substantial motility of virus-binding macrophages by MP-IVM, at least during the first 6 h after challenge. Viral particles therefore most probably reached the lymph node parenchyma by moving along the macrophage surface. VSV and other antigens are also presented to B cells by dendritic cells immigrating from peripheral locations[12,13], but footpad-derived dendritic cells are not likely to have a function during these very early events because their migration into popliteal lymph nodes takes much longer. We conclude that the SCS floor is not insurmountable for lymph-borne viruses; $CD169^+$ macrophages seem to act as gatekeepers and facilitators of viral translocation and presentation to B cells.

Next, we explored how naive B cells respond to viral encounter by using two VSV serotypes, Indiana (VSV-IND) and New Jersey (VSV-NJ) (Supplementary Fig. 6)[14]. We compared wild-type B cells with B cells from VI10YEN mice, which express a VSV-IND-specific B cell receptor that does not bind VSV-NJ[15]. By contrast, a small fraction (2–5%) of wild-type B cells bound both serotypes without being activated. This might reflect low-affinity reactivity with VSV surface glycoprotein or indirect interactions, for example through complement[16]. To assess B cell responses *in vivo*, differentially labelled wild-type and VI10YEN B cells were adoptively transferred and allowed to home to lymph node follicles. Fluorescent ultraviolet-inactivated virus was then injected into footpads, and popliteal lymph nodes were recorded by MP-IVM about 5–35 min later. In virus-free lymph nodes (Supplementary Movie 4) or after injection of VSV-NJ (Supplementary Movie 5), VI10YEN and control B cells had the same distribution (Fig. 2b, c). In contrast, on injection of VSV-IND, VI10YEN cells rapidly accumulated below and within the SCS floor (Supplementary Movie 6). There was no difference in baseline B-cell motility and distribution between CLL-treated and untreated lymph nodes, suggesting that VSV-specific B cells are equally likely to probe the SCS in both conditions (not shown). However, in CLL-treated lymph nodes, fluorescent virus was not retained in the SCS, and VI10YEN B cells failed to congregate in that region, indicating that SCS macrophages are essential for both events (Fig. 2b, Supplementary Movie 7).

To quantify VI10YEN B-cell distribution rigorously, lymph nodes were harvested 30 min after challenge with VSV and analysed by confocal microscopy. Although the entire follicular VI10YEN population retained its overall distribution (Fig. 2d), the subset of cells residing 50 μm or less below the SCS shifted towards the SCS in VSV-IND-containing, but not VSV-NJ-containing, lymph nodes (Fig. 2e). It seems unlikely that VI10YEN B cells redistributed to

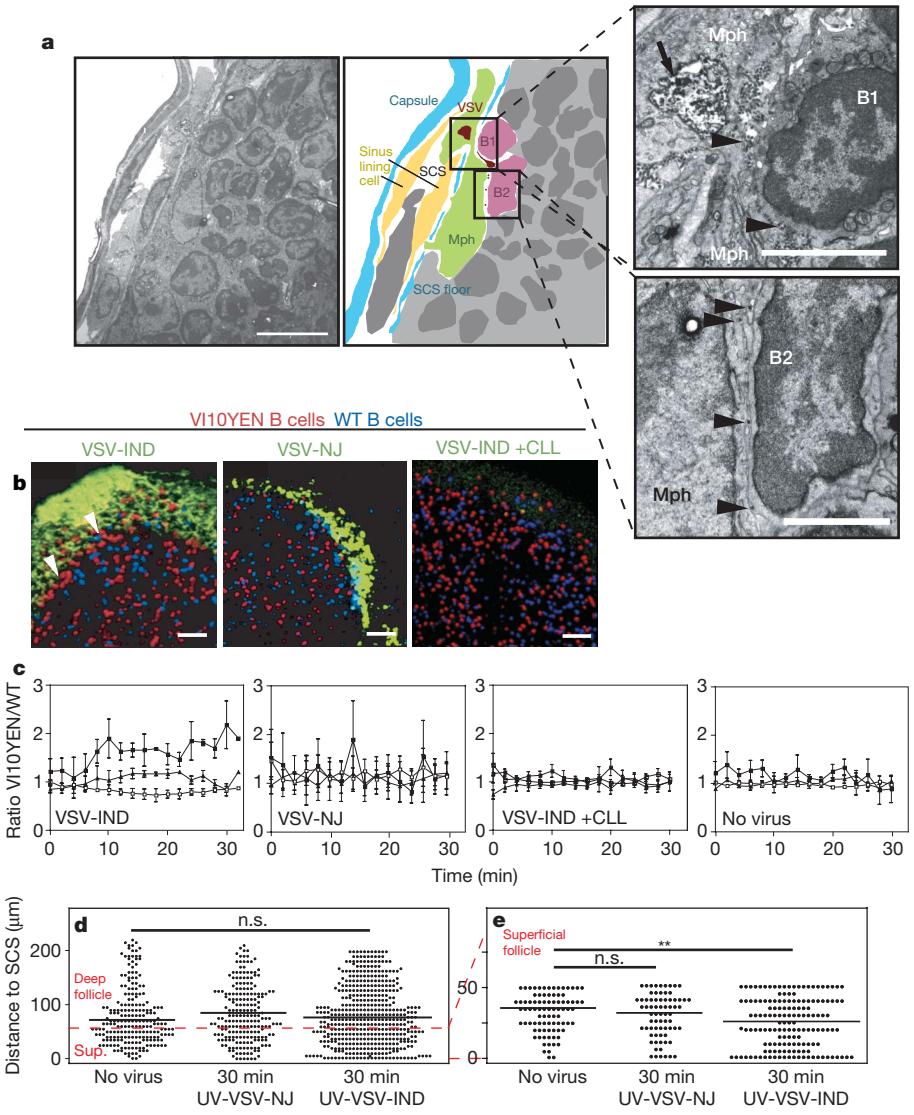

Figure 2 | Macrophage-mediated transfer of lymph-borne VSV across the SCS floor alters virus-specific B cell behaviour. **a**, Electron micrographs and schematic drawing (middle) showing a macrophage (Mph) penetrating the SCS floor of a popliteal lymph node 30 min after injection of VSV. Scale bars, 10 μm (left), 4 μm (right). The arrow indicates a vacuole with digested VSV; arrowheads indicate virions in the contact zone between the macrophage and B cells. **b**, MP-IVM of polyclonal (blue) and VI10YEN B cells (red) in popliteal lymph nodes. WT, wild type. Scale bars, 50 μm. **c**, Regional ratios of VI10YEN B cells/control B cells after VSV injection. Results are from three movies per group. Filled squares, subcapsular sinus; filled triangles, superficial follicle; open squares, deep follicle. Error bars indicate s.e.m. **d**, **e**, Localization of VI10YEN B cells in popliteal lymph nodes relative to the SCS in the entire follicle (**d**) and in the superficial follicle (**e**). Two asterisks, $P < 0.01$ (one-way ANOVA with Bonferroni's post-test); n.s., not significant; sup., superficial follicle; UV-VSV, ultraviolet-inactivated VSV. Horizontal bars in **d** and **e** indicate medians.

the SCS because of chemoattractant signals, because unresponsive polyclonal B cells express the same chemoattractant receptors. It is more likely that the random contacts of motile VI10YEN cells with macrophage-bound VSV-IND triggered a B-cell receptor (BCR)-dependent 'stop signal'[17]: short-term exposure to VSV-IND activates LFA-1 and/or α4 integrins[18] on VI10YEN B cells, resulting in adhesion to the respective ligands, intercellular cell-adhesion molecule-1 (ICAM-1) and vascular cell adhesion molecule-1 (VCAM-1), which are both expressed in the SCS (Supplementary Fig. 7). In addition, VSV-IND bound to SCS macrophages may provide a substrate for VI10YEN B-cell adhesion directly by means of the BCR.

To investigate how captured virions are processed on detection by B cells, we tested B cells from VI10YEN × MHCII-EGFP mice, which allowed us to detect endocytosed VSV colocalizing with endosomal MHC-II as an indicator of B-cell priming[19]. Within 30 min after injection, VI10YEN × MHCII-EGFP B cells in the superficial follicle had extensively internalized VSV-IND but not VSV-NJ particles (Fig. 3a, b, Supplementary Movie 8, and data not shown). Virus-carrying VSV-specific B cells were infrequent but detectable in deep follicles. These cells may have acquired virions from rare polyclonal B cells that carried VSV on their surface (not shown), or they may correspond to VI10YEN cells that failed to arrest at the SCS after acquiring VSV-IND.

Although our histological findings show that intact virions are preferentially detected and acquired by B cells in the SCS and superficial follicle, MP-IVM measurements of B-cell motility revealed broader antigen dissemination. After injection of VSV-IND, VI10YEN cells responded with a rapid decrease in velocity throughout the entire B follicle (Supplementary Fig. 8). This was observed equally in CLL-treated and control lymph nodes, indicating that viral antigen reached B cells independently of macrophages. This antigenic material was most probably composed of free viral protein, an inevitable by-product of natural infections. Indeed, purified supernatant of our VSV stocks induced a potent Ca^{2+} flux in VI10YEN B cells (Supplementary Fig. 6e). Small lymph-borne proteins are known to diffuse rapidly into follicles and activate cognate B cells[20]. Accordingly, injection of viral supernatant suppressed the motility of follicular VI10YEN B cells without inducing their accumulation at the SCS (not shown), indicating that free VSV surface glycoprotein was contained and active within the viral inoculum. This can explain the macrophage-independent pan-follicular effect of VSV-IND injection.

To determine the kinetics of VI10YEN B cell activation on viral encounter, we measured common activation markers (Supplementary Fig. 9). The co-stimulatory molecule CD86 was first upregulated 6 h after VSV-IND challenge. CD69 was induced more rapidly, but also on polyclonal B cells, presumably by pleiotropic interferon-α signalling[21,22]. Surface IgM (Fig. 3c, d) was downregulated as early as 30 min after challenge, reaching minimum levels within 2 h when more than 70% of VI10YEN cells were $BCR^{low/neg}$. BCR internalization therefore provided the earliest specific readout for virus-specific B-cell activation. VI10YEN B cells in CLL-treated lymph nodes failed to downregulate their BCR during the first 2 h after subcutaneous injection of 20 μg of VSV-IND (Fig. 3e), indicating that SCS macrophages are necessary for efficient early presentation of captured virions to B cells.

Primed B cells eventually solicit help from $CD4^+$ T cells[19] for class switch recombination and germinal centre formation. To contact T

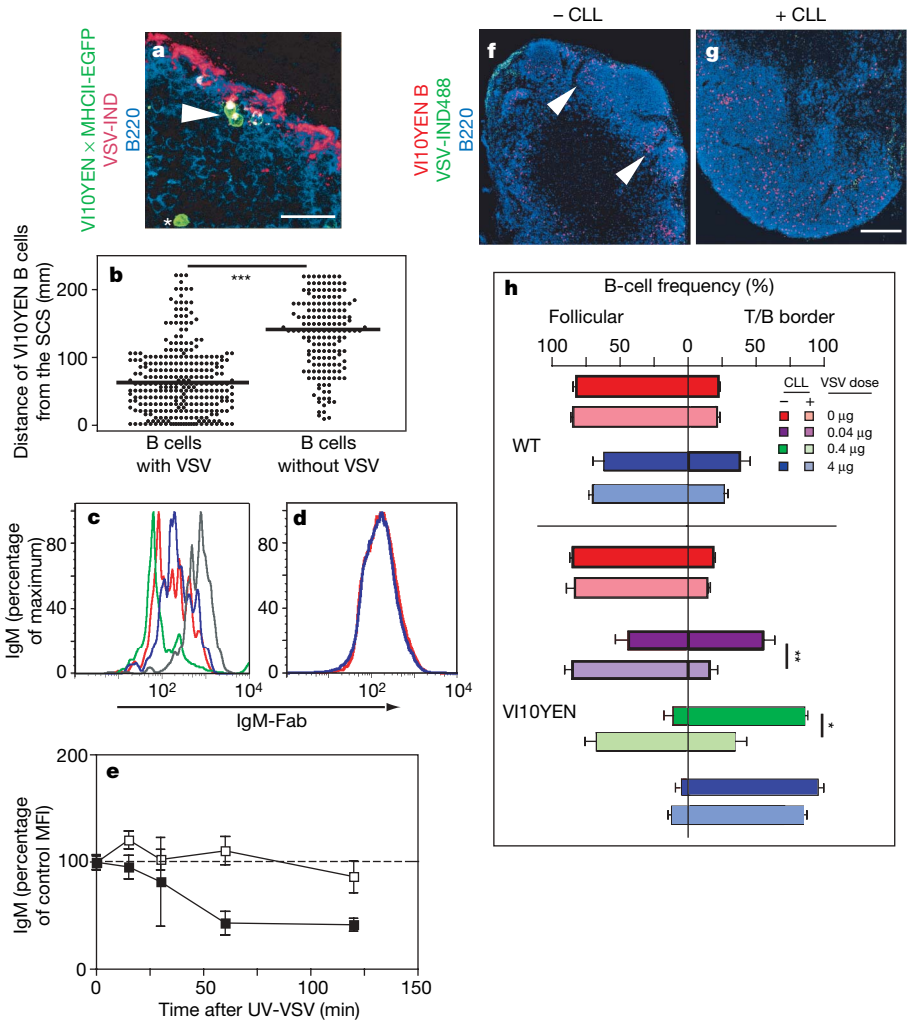

Figure 3 | SCS macrophages are required for early activation of VSV-specific B cells in lymph nodes. **a**, Confocal micrograph showing MHC-II (green) colocalization with VSV-IND (red; 30 min after injection) in VI10YEN × MHCII-EGFP B cells at the SCS (arrowhead) but not the deep follicle (asterisk). Scale bar, 25 μm. **b**, Distance of VSV-associated and VSV-free VI10YEN × MHCII-EGFP B cells to the SCS. Horizontal lines indicate medians; three asterisks, $P < 0.001$. **c**, **d**, BCR expression kinetics on VI10YEN cells (**c**) and polyclonal B cells (**d**) after injection of VSV-IND into the footpad. In **c**: dark grey, no virus; blue, 30 min; red, 1 h; green, 2 h. In **d**: red, no virus; blue, 2 h after treatment with ultraviolet-inactivated VSV. **e**, Expression of BCR on VI10YEN cells in CLL-treated (open squares) and untreated (filled squares) popliteal lymph nodes after injection of VSV-IND (20 μg). Mean fluorescence intensities were normalized to virus-free values (dashed line). UV-VSV, ultraviolet-inactivated VSV. Results are means ± s.e.m. (three to five mice). **f**, **g**, Confocal micrograph of VI10YEN B cells in control (**f**) and CLL-treated popliteal (**g**) lymph nodes 6 h after injection of VSV-IND (0.4 μg). Scale bar, 125 μm. **h**, Wild-type (WT) and VI10YEN B-cell frequency at T/B borders and in follicles of intact and CLL-depleted lymph nodes, 6 h after injection of VSV-IND. Bars depict the relative frequencies of transferred WT B cells (upper four bars) and VI10YEN cells (lower eight bars) in the two follicular compartments. Colour coding indicates injected doses of ultraviolet-inactivated VSV into CLL-treated recipients (light colours) or untreated recipients (dark colours). Error bars indicate s.e.m. $n = 3$–4 follicles per two mice; asterisk, $P < 0.05$; two asterisks, $P < 0.01$; three asterisks, $P < 0.001$ (*t*-test).

cells, newly activated B cells migrate towards the T/B border[17,23]. This mechanism operated efficiently in macrophage-sufficient mice: most VI10YEN B cells redistributed to the T/B border within 6 h after injection of as little as 40 ng of VSV-IND into the footpad (Fig. 3f, h, and Supplementary Fig. 10). By contrast, a 100-fold higher viral dose was needed to elicit full redistribution of VI10YEN B cells in CLL-treated mice (Fig. 3g, h). By 12 h after injection, most VSV-specific cells reached the T/B border, irrespective of the injected dose. Thus, even without SCS macrophages, follicular B cells are eventually activated by VSV-derived antigen, although less efficiently.

Thus, we have shown a dual role for $CD169^+$ macrophages in lymph nodes: they capture lymph-borne viruses preventing their systemic dissemination and they guide captured virions across the SCS floor for the efficient presentation and activation of follicular B cells.

METHODS SUMMARY

VSV-IND and VSV-NJ virions were purified from culture supernatants of infected BSRT7 cells and used either unmodified or fluorescently labelled with Alexa568 (red) or Alexa488 (green). Fluorescent viruses used for tissue imaging were irradiated with ultraviolet light to prevent the generation of non-fluorescent progeny. Fluorescent labelling or ultraviolet irradiation of VSV-IND particles did not affect their antigenicity or their ability to elicit a Ca^{2+} flux in VI10YEN cells (not shown). After injection of fluorescent virus into footpads, draining popliteal lymph nodes were harvested for analysis by electron microscopy or to generate frozen sections for immunostaining and confocal microscopy. To image adoptively transferred B cells in lymph nodes, VI10YEN and wild-type B cells were fluorescently labelled and transferred together by intravenous injection into wild-type or mutant recipient mice. After 18 h, when B cells had homed to B cell follicles, mice were injected with labelled or unlabelled VSV in the right footpad. At different time intervals thereafter, the draining popliteal lymph node was observed by MP-IVM or harvested for confocal microscopy or for flow cytometry to analyse the activation state of virus-specific and control B cells. In some experiments, macrophages in the popliteal lymph node were depleted by subcutaneous injections of CLL, and animals were used for experiments seven to ten days later. MP-IVM, electron microscopy, immunohistochemistry and flow cytometry for various markers were performed on lymph nodes with and without previous CLL treatment. Propagation of VSV from the footpad injection site to the blood and other organs was assessed by injecting a defined amount of live VSV into footpads followed by tissue harvest at 2 or 6 h after VSV injection. To measure viral titres, tissues were homogenized and used in plaque assays. Some viral propagation experiments were performed after cannulation of the thoracic duct.

Full Methods and any associated references are available in the online version of the paper at www.nature.com/nature.

Received 29 July; accepted 21 September 2007.
Published online 14 October 2007.

1. von Andrian, U. H. & Mempel, T. R. Homing and cellular traffic in lymph nodes. *Nature Rev. Immunol.* **3,** 867–878 (2003).
2. Karrer, U. *et al.* On the key role of secondary lymphoid organs in antiviral immune responses studied in alymphoplastic (aly/aly) and spleenless ($Hox11^{-/-}$) mutant mice. *J. Exp. Med.* **185,** 2157–2170 (1997).
3. Mead, D. G., Ramberg, F. B. & Mare, C. J. Laboratory vector competence of black flies (Diptera: Simuliidae) for the Indiana serotype of vesicular stomatitis virus. *Ann. NY Acad. Sci.* **916,** 437–443 (2000).
4. Bachmann, M. F., Hengartner, H. & Zinkernagel, R. M. T helper cell-independent neutralizing B cell response against vesicular stomatitis virus: role of antigen patterns in B cell induction? *Eur. J. Immunol.* **25,** 3445–3451 (1995).
5. Mempel, T. R., Henrickson, S. E. & von Andrian, U. H. T-cell priming by dendritic cells in lymph nodes occurs in three distinct phases. *Nature* **427,** 154–159 (2004).
6. Clark, S. L. Jr. The reticulum of lymph nodes in mice studied with the electron microscope. *Am. J. Anat.* **110,** 217–258 (1962).
7. Farr, A. G., Cho, Y. & De Bruyn, P. P. The structure of the sinus wall of the lymph node relative to its endocytic properties and transmural cell passage. *Am. J. Anat.* **157,** 265–284 (1980).
8. Ochsenbein, A. F. *et al.* Protective T cell-independent antiviral antibody responses are dependent on complement. *J. Exp. Med.* **190,** 1165–1174 (1999).
9. Ochsenbein, A. F. *et al.* Control of early viral and bacterial distribution and disease by natural antibodies. *Science* **286,** 2156–2159 (1999).
10. Taylor, P. R. *et al.* Macrophage receptors and immune recognition. *Annu. Rev. Immunol.* **23,** 901–944 (2005).
11. Delemarre, F. G., Kors, N., Kraal, G. & van Rooijen, N. Repopulation of macrophages in popliteal lymph nodes of mice after liposome-mediated depletion. *J. Leukoc. Biol.* **47,** 251–257 (1990).
12. Ludewig, B. *et al.* Induction of optimal anti-viral neutralizing B cell responses by dendritic cells requires transport and release of virus particles in secondary lymphoid organs. *Eur. J. Immunol.* **30,** 185–196 (2000).
13. Qi, H., Egen, J. G., Huang, A. Y. & Germain, R. N. Extrafollicular activation of lymph node B cells by antigen-bearing dendritic cells. *Science* **312,** 1672–1676 (2006).
14. Roost, H. P., Haag, A., Burkhart, C., Zinkernagel, R. M. & Hengartner, H. Mapping of the dominant neutralizing antigenic site of a virus using infected cells. *J. Immunol. Methods* **189,** 233–242 (1996).
15. Hangartner, L. *et al.* Antiviral immune responses in gene-targeted mice expressing the immunoglobulin heavy chain of virus-neutralizing antibodies. *Proc. Natl Acad. Sci. USA* **100,** 12883–12888 (2003).
16. Rossbacher, J. & Shlomchik, M. J. The B cell receptor itself can activate complement to provide the complement receptor 1/2 ligand required to enhance B cell immune responses *in vivo. J. Exp. Med.* **198,** 591–602 (2003).
17. Okada, T. *et al.* Antigen-engaged B cells undergo chemotaxis toward the T zone and form motile conjugates with helper T cells. *PLoS Biol.* **3,** e150 (2005).
18. Dang, L. H. & Rock, K. L. Stimulation of B lymphocytes through surface Ig receptors induces LFA-1 and ICAM-1-dependent adhesion. *J. Immunol.* **146,** 3273–3279 (1991).
19. Vascotto, F. *et al.* Antigen presentation by B lymphocytes: how receptor signaling directs membrane trafficking. *Curr. Opin. Immunol.* **19,** 93–98 (2007).
20. Pape, K. A., Catron, D. M., Itano, A. A. & Jenkins, M. K. The humoral immune response is initiated in lymph nodes by B cells that acquire soluble antigen directly in the follicles. *Immunity* **26,** 491–502 (2007).
21. Barchet, W. *et al.* Virus-induced interferon α production by a dendritic cell subset in the absence of feedback signaling *in vivo. J. Exp. Med.* **195,** 507–516 (2002).
22. Shiow, L. R. *et al.* CD69 acts downstream of interferon-α/β to inhibit S1P1 and lymphocyte egress from lymphoid organs. *Nature* **440,** 540–544 (2006).
23. Reif, K. *et al.* Balanced responsiveness to chemoattractants from adjacent zones determines B-cell position. *Nature* **416,** 94–99 (2002).

Supplementary Information is linked to the online version of the paper at www.nature.com/nature.

Acknowledgements We thank G. Cheng, M. Flynn and D. Baumjohann for technical support; R. M. Zinkernagel and H. Hengartner for providing VI10YEN mice; A. Wagers for providing Act(EGFP) mice; M. Ericsson and E. Benecchi for expert support in electron microscopy studies; S. Behnke for immunohistochemistry; and D. Cureton for help and advice with VSV preparations. This work was supported by grants from the NIH-NIAID (to U.H.v.A.), a Pilot and Feasibility Grant from the Harvard Skin Disease Research Center (to T.J. and U.H.v.A.), a stipend from the Swiss National Science Foundation (to T.J.) and a NIH T32 Training Grant in Hematology (to E.A.M.).

Author Contributions T.J. and U.H.v.A. designed the study; T.J., E.A.M., M.I., S.M. and P.A.L. performed experiments; T.J., E.A.M., M.I. and S.M. collected and analysed data; M.B., K.F., N.C.D.P., D.M.S., N.v.R. and S.P.W. provided reagents and mice; T.J., E.A.M., M.I. and U.H.v.A. wrote the manuscript; S.M., K.F., S.E.H., T.M. and S.P.W. gave technical support and conceptual advice.

Author Information Reprints and permissions information is available at www.nature.com/reprints. Correspondence and requests for materials should be addressed to U.V.A. (uva@hms.harvard.edu).

METHODS

Mice and antibodies. C57BL/6 and BALB/c mice were purchased from Taconic Farms. VI10YEN[15], $C3^{-/-}$ (ref. 24), MHCII-EGFP[25], Act(EGFP)[26] and DH-LMP2A mice[27] were bred in barrier animal facilities at Harvard Medical School and the Immune Disease Institute (IDI). Radiation chimaeras were generated by irradiation of Act(EGFP) mice with two doses of 650 rad and reconstitution with C57BL/6 bone marrow, and were allowed to reconstitute for eight weeks before use. In some experiments, SCS macrophages were depleted by footpad injections of 30 µl clodronate liposomes (CLL), seven to ten days before the experiment. Clodronate was a gift from Roche Diagnostics GmbH. Other reagents for preparation of liposomes were phosphatidylcholine (LIPOID E PC; Lipoid GmbH) and cholesterol (Sigma-Aldrich). Mice were housed under specific pathogen-free and antiviral antibody-free conditions in accordance with National Institutes of Health guidelines. All experimental animal procedures were approved by the Institutional Animal Committees of Harvard Medical School and the IDI. Antibodies were purchased from BD Biosciences, except anti-B220-Alexa647 (Invitrogen-Caltag), anti-LYVE-1 (Millipore-Upstate), goat anti-rabbit–APC (Invitrogen), goat anti-GFP–FITC (Rockland), anti-FITC-Alexa488 (Invitrogen) and Fab anti-IgM-FITC (Jackson Immunoresearch). The following antibodies were purchased from AbD-Serotec: anti-CD68-Alexa647, anti-CD11b-Alexa647, F4/80-Alexa647 and anti-CD169-FITC (3D6). The anti-idiotypic antibody 35.61 for detection of the VI10 BCR in VI10YEN mice[15] was produced from hybridoma supernatants in accordance with standard methods.

Flow cytometry. Flow cytometric analysis of blood samples was performed after retro-orbital phlebotomy of mice and lysis of erythrocytes with ACK buffer (0.15 M NH_4Cl, 1 mM $KHCO_3$, 0.1 mM EDTA (disodium salt), pH 7.2). Single-cell suspensions of lymph nodes and spleens for flow cytometry were generated by careful mincing of tissues and subsequent digestion at 37 °C for 40 min in DMEM (Invitrogen-Gibco) in the presence of 250 µg ml^{-1} liberase CI (Roche) plus 50 µg ml^{-1} DNase I (Roche). After 20 min of digestion, samples were passed vigorously through an 18-gauge needle to ensure complete organ dissociation. All flow cytometric analyses were performed in FACS buffer containing PBS with 2 mM EDTA and 2% FBS (Invitrogen-Gibco) on a FACScalibur (BD Pharmingen), and analysed by FlowJo software (Treestar Inc.). For Ca^{2+} flux, cells were labelled for 90 min at 37 °C with 4 µM Fluo-LOJO (Teflabs) in DMEM containing 10% FCS. Cells were spun through FCS and used immediately.

Viruses and VSV plaque assay. VSV, serotypes Indiana (VSV-IND; Mudd-Summers-derived clone, *in vitro* rescued[28] and plaque purified) or New Jersey (VSV-NJ; Pringle Isolate, plaque purified) were propagated at a multiplicity of infection (m.o.i.) of 0.01 on BSRT7 cells. Supernatants of infected cells were cleared from cell debris by centrifugation at 2,000*g*, filtered through 0.45-µm sterile filters and subjected to ultracentrifugation at 40,000*g* for 90 min. Pellets were resuspended in PBS and purified by ultracentrifugation (157,000*g*, 60 min) through a cushion of 10% sucrose in NTE buffer (0.5 mM NaCl, 10 mM Tris-HCl pH 7.5, 5 mM EDTA pH 8). After resuspension overnight in PBS, virus protein was quantified by bicinchoninic acid assay (Pierce), and infectivity was quantified by plaque assay. Some batches were labelled with carboxylic acid succinimidyl esters of AlexaFluor-488 or AlexaFluor-568 (Invitrogen-Molecular Probes) at a 10^4–10^5-fold molar excess of Alexa dye over virus particles. Unconjugated dye was removed by ultracentrifugation through 10% sucrose in NTE buffer; pellets were resuspended in PBS and stored frozen. Infectivity of VSV preparations was quantified by plaque assay on green monkey kidney cells (Vero). VSV titres from organs of infected mice were determined similarly, after homogenization of the organs with a Potter–Elvehjem homogenizer. When necessary, during viral preparation, the roughly 4-ml supernatants from the 157,000*g* ultracentrifugation were collected and concentrated with a 10-kDa molecular mass cut-off Amicon Ultra (Millipore). To account for residual infectivity in concentrated supernatants, VSV stocks were diluted to levels of infectivity equal to that of the concentrated supernatants, and the Ca^{2+} flux in VI10YEN B cells was compared over further 100-fold dilutions of VSV and supernatant. Ultraviolet-inactivated, AlexaFluor-568-labelled adenovirus 5 was generated in accordance with standard procedures[29]. All work on infectious materials was performed in designated BL2+ workspaces, in accordance with institutional guidelines, and approved by the Harvard Committee on Microbiological Safety.

VSV neutralization assay. Serum from immunized mice was prediluted 40-fold in MEM containing 2% FCS. Serial twofold dilutions were mixed with equal volumes of VSV (500 plaque-forming units ml^{-1}) and incubated for 90 min at 37 °C in 5% CO_2. Serum–virus mixture (100 µl) was transferred to Vero cell monolayers in 96-well plates and incubated for 1 h at 37 °C. The monolayers were overlaid with 100 µl of DMEM containing 1% methylcellulose and incubated for 24 h at 37 °C. Subsequently, the overlay was discarded and the monolayer was fixed and stained with 0.5% crystal violet. The highest dilution of serum that decreased the number of plaques by 50% was taken as the titre. To determine IgG titres, undiluted serum was pretreated with an equal volume of 0.1 mM 2-mercaptoethanol in saline solution.

Adhesion assays. Corning 96-well plates were coated overnight with dilutions of recombinant murine VCAM-1-Fc or ICAM-1-Fc (R&D Systems) or with purified VSV-IND in PBS in triplicate. Negative control wells were coated with 4% BSA, positive control wells were coated with 1 mg ml^{-1} poly-(L-lysine). Plates were blocked for 1–2 h at 4 °C with HBSS/1% BSA and washed. Naive B cells from VI10YEN or C57BL/6 mice were negatively selected by magnetic cell separation with CD43 magnetic beads (Miltenyi) and added to the plates at 3×10^5 per well in HBSS with 1% BSA, 1 mM Ca^{2+} and 1 mM Mg^{2+} in the presence or absence of ultraviolet-inactivated VSV-IND (m.o.i. 1,000) for 30 min at 37 °C. After gentle washing three, times in HBSS with 1% BSA), plates were fixed for 10 min with PBS/10% glutaraldehyde, stained for 45 min with 0.5% crystal violet/20% methanol and washed in water. The dye was eluted by addition of 1% SDS and the absorbance at 570 nm was determined spectrophotometrically (SpectraMax340PC microplate reader and SoftmaxPro 3.1.2 software; Molecular Devices Corporation) after 30 min.

Confocal microscopy. For some analyses, both hind footpads of C57BL/6 mice were injected with 20 µg of AlexaFluor-568-labelled or AlexaFluor-488-labelled VSV-IND or VSV-NJ and the draining lymph nodes were harvested after 30 min. For other experiments, mice were transfused with 10^7 negatively selected naive B cells from VI10YEN × MHCII-EGFP mice one day before the experiment. At predetermined time points, popliteal lymph nodes were fixed *in situ* by footpad injections of phosphate-buffered L-lysine with 1% paraformaldehyde/periodate (PLP). After removal of popliteal lymph nodes and incubation for 3–5 h in PLP at 4 °C, popliteal lymph nodes were washed in 0.1 M PBS pH 7.2 and cryoprotected by an ascending series of 10%, 20% and 30% sucrose in PBS. Samples were snap-frozen in TBS tissue-freezing liquid (Triangle Biomedical Sciences) and stored at −80 °C. Sections of 40 µm thickness were mounted on Superfrost Plus slides (Fisherbrand) and stained with fluorescent antibodies in a humidified chamber after Fc receptor blockade with 1 µg ml^{-1} antibody 2.4G2 (BD Pharmingen). Samples were mounted in FluorSave reagent solution (EMD-Calbiochem) and stored at 4 °C until analysis. Images were collected with a Bio-Rad confocal microscopy system using an Olympus BX50WI microscope and 10×/0.4 numerical aperture or 60×/1.2 numerical aperture water-immersion objective lenses. Images were analysed with LaserSharp2000 software (Bio-Rad Cell Science) and Photoshop CS (Adobe). Quantification of B cells localized at the T/B border was done by counting cells that were within 50 µm of the T/B border, as denoted by B220 counterstain; any cells localized in more central regions were considered follicular.

Electron microscopy. Popliteal lymph nodes were fixed *in situ* by footpad injection of 2% formaldehyde and 2.5% glutaraldehyde in 0.1 M sodium cacodylate buffer pH 7.4. The lymph nodes were excised and immersed in the same buffer overnight at 4 °C, washed in cacodylate buffer and osmicated with 1% osmium tetroxide/1.5% potassium ferrocyanide (in water) for 1 h at 18–22 °C in the dark. After being washed in water, samples were washed three or four times in 0.05 M maleate buffer pH 5.15. Samples were counterstained for 2 h in 1% uranyl acetate in maleate buffer and washed three times in water. Samples were dehydrated by incubation for 15 min in dilutions of ethanol in water (70%, 90% and 100%), incubated in propylene oxide for 1 h and transferred into Epon mixed 1:1 with propylene oxide at room temperature overnight. Samples were moved to an embedding mould filled with freshly mixed Epon, and heated for 24–48 h at 60 °C for polymerization. Samples were analysed on a Tecnai G2 Spirit BioTWIN electron microscope at the Harvard Medical School electron microscope facility.

Intravital MP-IVM of the popliteal lymph node. Naive B cells were negatively selected by magnetic isolation with CD43 beads (Miltenyi). VI10YEN B cells were labelled for 20 min at 37 °C with 10 µM 5-(and 6-)-(((4-chloromethyl) benzoyl)amino)tetramethylrhodamine (CMTMR; Invitrogen), C57BL/6 B cells were labelled for 25 min at 37 °C with 10 µM 7-amino-4-chloromethylcoumarin (CMAC; Invitrogen). In some experiments, labels were swapped between wild-type and VI10YEN B cells to exclude unspecific dye effects (data not shown). B cells ($(5–6) \times 10^6$) from each population were mixed and adoptively transferred by tail-vein injection into C57BL/6 recipient mice one day before analysis. In some experiments, recipient C57BL/6 mice had received an injection of 30 µl of CLL into the hind footpad 7–10 days before the experiment to eliminate SCS macrophages[11]. At 18 h after adoptive B-cell transfer, recipient mice were anaesthetized by intraperitoneal injection of ketamine (50 mg kg^{-1}) and xylazine (10 mg kg^{-1}). The right popliteal lymph node was prepared microsurgically for MP-IVM and positioned on a custom-built microscope stage as described[5]. Care was taken to spare blood vessels and afferent lymph vessels. The exposed lymph node was submerged in normal saline and covered with a glass coverslip. A thermocouple was placed next to the lymph node to monitor local temperature, which was maintained at 36–38 °C. MP-IVM was performed on a Bio-Rad

2100MP system at an excitation wavelength of 800 nm, from a tunable MaiTai Ti:sapphire laser (Spectra-Physics). Fluorescently labelled VSV (20 μg in 20 μl) was injected through a 31-gauge needle into the right hind footpad of recipient mice concomitant to observation. For four-dimensional offline analysis of cell migration, stacks of 11 optical *x*–*y* sections with 4-μm *z* spacing were acquired every 15 s with electronic zooming to ×1.8–3.0 through a 20×/0.95 numerical aperture water-immersion objective lens (Olympus). Emitted fluorescence and second-harmonic signals were detected through 400/40 nm, 450/80 nm, 525/50 nm and 630/120 nm bandpass filters with non-descanned detectors to generate three-colour images. Sequences of image stacks were transformed into volume-rendered, four-dimensional time-lapse movies using Volocity software (Improvision). Three-dimensional instantaneous velocities were determined by semi-automated cell tracking with Volocity and computational analysis by Matlab (Mathworks). Accumulation of cells at the SCS was determined by manual movie analysis performed by blinded observers. Every 2 min, the VI10YEN B cells and polyclonal B cells were counted at the SCS, in the superficial follicle (less than 50 μm distance from the SCS) and the deep follicle (more than 50 μm distance from the SCS), and ratios of VI10YEN/polyclonal B cells were expressed for each compartment in the entire 30-min movie.

Thoracic duct cannulation. For thoracic duct cannulation, mice received 200 μl of olive oil by gavage 30 min before cannulation to facilitate visualization of the lymph vessels. Animals were then anaesthetized with xylazine (10 mg kg^{-1}) and ketamine HCl (50 mg kg^{-1}). A polyethylene catheter (PE-10) was inserted into the right jugular vein for continuous infusion (2 ml h^{-1}) of Ringer's lactate (Abbott Laboratories) containing 1 U ml^{-1} heparin (American Pharmaceutical Partners). With the use of a dissecting microscope, the thoracic duct was exposed through a left subcostal incision. Silastic silicon tubing (0.012 inch internal diameter; Dow Corning) was flushed with heparinized (50 U ml^{-1}) PBS (DPBS; Mediatech), inserted into the cisterna chyli through a roughly 0.3-mm incision and fixed with isobutyl cyanoacrylate monomer (Nexaband; Abbott Laboratories). The remaining part of the tubing was drawn to the exterior through the posterior abdominal wall. Subsequently, the abdominal incision was closed with a 6-0 nonabsorbable running suture (Sofsilk; Tyco Healthcare Group). After equilibration of lymph flow for 30 min, animals were injected into the footpad with 10^8 plaque-forming units of VSV-IND and lymph samples were collected on ice for 6 h. Blood and organs were taken after 6 h of collection of thoracic duct lymph and plaque-assayed as described above. Lymph and organs were plaque-assayed as described above. In some experiments the draining popliteal and para-aortic lymph nodes were surgically excised and the surrounding lymph vessels were cauterized to prevent lymph-borne viral access to the blood.

24. Wessels, M. R. *et al.* Studies of group B streptococcal infection in mice deficient in complement component C3 or C4 demonstrate an essential role for complement in both innate and acquired immunity. *Proc. Natl Acad. Sci. USA* **92,** 11490–11494 (1995).
25. Boes, M. *et al.* T-cell engagement of dendritic cells rapidly rearranges MHC class II transport. *Nature* **418,** 983–988 (2002).
26. Wright, D. E. *et al.* Cyclophosphamide/granulocyte colony-stimulating factor causes selective mobilization of bone marrow hematopoietic stem cells into the blood after M phase of the cell cycle. *Blood* **97,** 2278–2285 (2001).
27. Casola, S. *et al.* B cell receptor signal strength determines B cell fate. *Nature Immunol.* **5,** 317–327 (2004).
28. Whelan, S. P., Ball, L. A., Barr, J. N. & Wertz, G. T. Efficient recovery of infectious vesicular stomatitis virus entirely from cDNA clones. *Proc. Natl Acad. Sci. USA* **92,** 8388–8392 (1995).
29. Leopold, P. L. *et al.* Fluorescent virions: dynamic tracking of the pathway of adenoviral gene transfer vectors in living cells. *Hum. Gene Ther.* **9,** 367–378 (1998).